Influence of the number of cells for finite size artificial magnetic conductor

Céline Ha, Jean-François Pintos, Priscillia Daquin, Serge Bories

Influence of the Number of Cells for Finite Size Artificial Magnetic Conductor

Céline Ha[1*], Jean-François Pintos[1], Priscillia Daquin[2], Serge Bories[1]

[1]Univ. Grenoble Alpes, CEA, Leti, F-38000 Grenoble, France
[2]Antenna Department, CNES, F-31000, Toulouse, France
*corresponding author, E-mail: celine.ha@cea.fr

Abstract

This paper examines the influence of the cell number for finite size AMC under normal plane wave incidence. A comparison is carried out on the operational frequency, the fractional bandwidth, and the reflection coefficient magnitude between the finite size AMC and an infinite structure, for different cell numbers and for three different finite size screens.

1. Introduction

Artificial Magnetic Conductors (AMC) are usually characterized with infinite boundary conditions and under normal plane wave incidence. Their operational frequency is defined when the reflection phase is 0°. This in-phase reflection property has made possible the design of low-profile antenna [1]-[4]. The effect of the AMC size has been examined for a finite square structure compared to the infinite unit cell response [5], for various unit cells configurations [2], and for low-profile antennas with a dipole over an AMC by varying the total surface of the screen [1]-[3]. However, the choice of the number of cells for a given surface has not been studied in details to the best of our knowledge and various configurations were suggested for the smallest square AMC studied: 2 x 2 [4], 4 x 4 [5], 5 x 5 [2, 3], and 6 x 6 [1] unit cells.

In this paper, the influence of the cell number for a finite size AMC under normal plane wave incidence is investigated. The unit cell is a metallic square patch over a grounded substrate. For a given surface, the number of cells is increased and the size of the unit cell is reduced, but the operational frequency remains the same by tuning the capacitor value placed in series between each patch. Operational frequency, fractional bandwidth and reflection coefficient magnitude (Γ) are compared between the finite size AMC and the infinite structure, for different numbers of cells (N x N cells, $2<N<32$) and for three different finite size screens ($0.45\lambda_0$ x $0.45\lambda_0$, $0.63\lambda_0$ x $0.63\lambda_0$, $0.77\lambda_0$ x $0.77\lambda_0$,).

2. Reference unit cell and finite AMC structures

The unit cell is a metallic square patch over a grounded FR4 substrate ($\varepsilon_r = 4.4$, $\tan\delta = 0.02$), which height is $h = 19.9$ mm ($\lambda_0/42$). The gap between each patch is $g = 2.5$ mm ($\lambda_0/333$) and is kept constant regardless the number of cells. A lumped capacitor is placed in series between each patch edge and its value allows to tune the operating frequency while the size of the square patch is reduced. With infinite boundary conditions and under normal plane wave incidence, each unit cell is tailored to operate at 360 MHz ($\lambda_0 = 833.33$ mm). Three AMC sizes are considered. Their dimensions and simulated cell configurations are summarized in Table 1. Table 2 details the cell configuration, for different numbers of cells on surface S1 ($0.45\lambda_0$ x $0.45\lambda_0$).

Table 1: Examined AMC structures.

Surface	Size [λ_0xλ_0]	Configurations
S1	0.45 x 0.45	3 x 3 to 24 x 24
S2	0.63 x 0.63	4 x 4 to 32 x 32
S3	0.77 x 0.77	5 x 5 to 30 x 30

Table 2: Unit cell dimension and capacitor value for surface S1.

Configu-ration	Patch edge size [mm]	Periodicity [mm]	Capacitor value [pF]
3 x 3	125.00 (λ_0/6.7)	127.50 (λ_0/6.5)	0
6 x 6	61.25 (λ_0/13.6)	63.75 (λ_0/13.1)	3.11
10 x 10	33.25 (λ_0/25.1)	35.75 (λ_0/23.3)	5.03
18 x 18	18.75 (λ_0/44.4)	21.25 (λ_0/39.2)	6.65

3. AMC properties and RCS

The AMC properties for finite size structures are retrieved from monostatic Radar Cross Section (RCS) method, under normal plane wave incidence. The reflection coefficient is related to the reflection coefficient through the equation (1) [6]:

$$\Gamma = 20\log\left(\sqrt{\frac{\sigma_{AMC}}{\sigma_{ref}}}\right) \qquad (1)$$

where Γ is the reflection coefficient in dB, σ_{AMC} is the RCS of the AMC in m², σ_{ref} is the RCS of the reference object in m². The reference plane considered here is a copper located at height h, and its size depends on the AMC under study (S1, S2 or S3). The AMC bandwidth is defined as the frequency bandwidth where the reflection phase is in the range ±90°.

4. Simulated results

As the surface of the AMC increases, the operating frequency of the finite AMC tends to decrease towards the frequency of the unit cell in infinite configuration: around 392 MHz for S1, 385 MHz for S2 and 375 MHz for S3, Figure 1. The operating frequency of the finite AMC is shifted to the highest frequency, as in [5]. As the surface is reduced, the operating frequency converges more quickly to its limit value, with less dense configurations: 12 x 12 cells for S3, 8 x 8 cells for S2 and 4 x 4 cells for S1. Increasing the number of cells does not enable the operating frequency to get closer to the tailored frequency. The fractional bandwidth of the finite AMC tends to increase towards the fractional bandwidth of the unit cell in infinite configuration as the AMC size increases, Figure 2. For the surfaces S2 and S3, the simulated results show that the bandwidth can be slightly better than the infinite case when the cells configuration is high, from 12 x 12 for S3 and from 20 x 20 for S2. The reflection coefficient magnitude indicates indirectly the level of energy absorbed by the AMC, Figure 3. The simulated results show that the finiteness of the AMC leads to lower reflection coefficient magnitude compared to the infinite unit cell configuration. As the number of cells increases for a given surface, the reflection coefficient magnitude increases, improving the AMC performances. For the finite AMC S2 and S3, the reflection level ceases to increase regarding the number of cells from 12 x 12 cells configuration. In the case of the surface S1, the curve tends on average to the maximum value of the reflection coefficient from 20 x 20 cells.

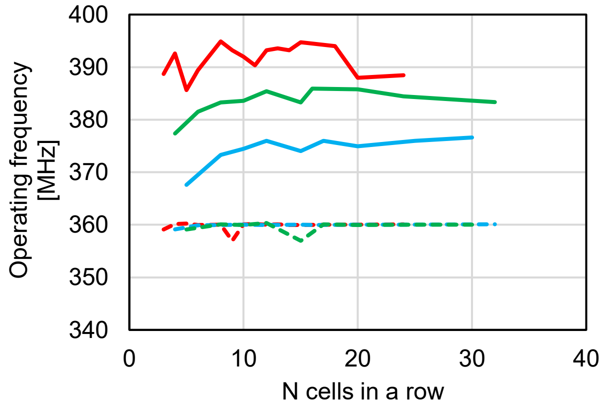

Figure 1: Operating frequency of the finite AMC depending on N^2 cells configuration for S1 (red), S2 (green) and S3 (blue), compared to infinite unit cell configuration for S1 (dashed red), S2 (dashed green) and S3 (dashed blue).

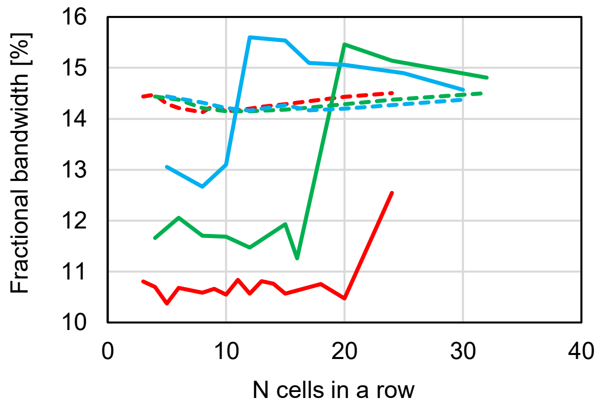

Figure 2: Fractional bandwidth of the finite AMC depending on N^2 cells configuration for S1 (red), S2 (green) and S3 (blue), compared to infinite unit cell configuration for S1 (dashed red), S2 (dashed green) and S3 (dashed blue).

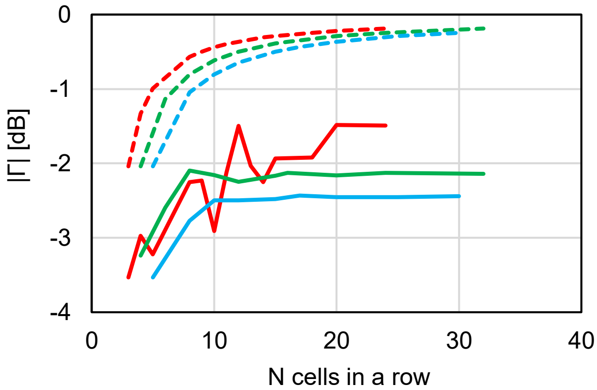

Figure 3: Reflection coefficient magnitude of the finite AMC depending on N^2 cells configuration for S1 (red), S2 (green) and S3 (blue), compared to infinite unit cell configuration for S1 (dashed red), S2 (dashed green) and S3 (dashed blue).

5. Conclusions

The number of cells and the size of an AMC have an influence on the operating frequency, the fractional bandwidth and the reflection coefficient magnitude of the AMC. As the surface of the AMC may be constrained by size requirements, the number of cells can be considered as a parameter to modify the performance of the AMC. A small number of cells induces a lower reflection coefficient magnitude, therefore higher energy absorbed by the AMC, and a lower bandwidth compare to the infinite cells structure. A higher number of cells enables to get closer to and even to exceed the bandwidth of the infinite cells case, depending on the size of the AMC. However, within the framework of reconfigurable metasurface by means of tunable capacitors, increasing the number of cells leads to enhance the complexity of the metasurface and its control circuitry.

References

[1] G. Bianconi, F. Costa, S. Genovesi, and A. Monorchio, ‘Optimal Design of Dipole Antennas Backed by a Finite

High-Impedance Screen', PIER C, vol. 18, pp. 137–151, 2011, doi: 10.2528/PIERC10111204.

[2] F. Costa, O. Luukkonen, C. R. Simovski, A. Monorchio, S. A. Tretyakov, and P. M. de Maagt, 'TE Surface Wave Resonances on High-Impedance Surface Based Antennas: Analysis and Modeling', IEEE Trans. Antennas Propagat., vol. 59, no. 10, pp. 3588–3596, Oct. 2011, doi: 10.1109/TAP.2011.2163750.

[3] S.K. Hampel, I. Kiral, O. Schmitz and I. Rolfes, 'Influence of finite High-Impedance Surface dimensions on the characteristics of a planar printed dipole', Proceedings of the Fourth European Conference on Antennas and Propagation, Barcelona, Spain, pp. 1-4, 2010.

[4] Y.-S. Chen and T.-Y. Ku, 'A Low-Profile Wearable Antenna Using a Miniature High Impedance Surface for Smartwatch Applications', Antennas Wirel. Propag. Lett., vol. 15, pp. 1144–1147, 2016, doi: 10.1109/LAWP.2015.2496366.

[5] M. Alyahya, C. Balanis, C. Birtcher, H. N. Shaman, and W. A. Aloma, 'Impact on Reflection Phase by Different Geometrical Structures of AMCs for RCS Reduction', 2018 IEEE International Symposium on Antennas and Propagation & USNC/URSI National Radio Science Meeting, Boston, MA, USA, pp. 2331-2332, 2018.

[6] G. A. Barnhart, 'Evaluation of the Sensitivity of Radar Cross Section Predictions to Uncertainties in Material Characteristics', M.S. thesis, Fac. of Sch. of Eng., Air Force Inst. of Tech., Ohio (USA), 1995. [Online]. Available: https://apps.dtic.mil/sti/pdfs/ADA309420.pdf